

TWO-COMPONENT BENARD CONVECTION IN CYLINDERS

E. CRESPO and M. G. VELARDE*

U.N.E.D.-Fisica Fundamental, Apdo. Correos 50 487, Madrid, Spain

(Received 12 April 1982)

Abstract—A nonreactive binary (gas or liquid) mixture in a vertical cylinder heated from below is considered. Sufficient conditions are given for steady thermoconvective instability. Both axi- and asymmetric modes of convection are considered. The theoretical predictions are compared with the available experimental data.

NOMENCLATURE

D ,	mass diffusivity;
D'' ,	Onsager's Dufour cross-coefficient;
$\mathbf{e}_r, \mathbf{e}_\phi, \mathbf{e}_z$,	unit vectors;
f ,	aspect ratio, R/L ;
h ,	aspect ratio, $L/2R (= 1/2f)$;
I_n ,	n th order of modified Bessel function;
J_n ,	n th order of Bessel function;
k ,	solution of equation (2.7);
L ,	height of cylinder;
\mathbf{n} ,	outward unit normal vector;
N_1 ,	mass fraction of component one;
p ,	dimensionless pressure field;
P ,	Prandtl number, ν/κ ;
\tilde{P} ,	coefficient in pressure field representation;
r ,	dimensionless radial coordinate;
r_D ,	Lewis number, D/κ ;
S ,	Soret number, $\gamma\Delta N_1/(\alpha\Delta T)$;
t ,	dimensionless time;
T ,	dimensionless perturbation in temperature field;
ΔT ,	thermal gradient;
\mathbf{u} ,	velocity field;
u_r ,	radial component of dimensionless velocity;
U ,	coefficient in radial component of velocity field representation;
v ,	azimuthal component of dimensionless velocity;
w ,	vertical component of dimensionless velocity;
W ,	coefficient in radial component of velocity field representation;
z ,	dimensional vertical coordinate.

Greek symbols

α ,	thermal coefficient of expansion;
γ ,	volume expansion due to variation of the mass fraction N_1 ;
Γ ,	dimensionless perturbation in concentration field;
$\tilde{\Gamma}$,	coefficient in concentration field representation;

δ_1, δ_2 ,	see equations (2.15) and (2.16);
κ ,	thermal diffusivity;
μ_1 ,	chemical potential of component one;
ν ,	kinematic viscosity;
Ω ,	defined $T - \Gamma$;
ρ ,	density;
Ψ ,	defined $S(1 + D_F)/r_D(1 + S)(1 - D_F/r_D)$;
ϕ ,	azimuthal coordinate.

Superscripts

m ,	average;
c ,	critical.

INTRODUCTION

THE ROLE of Onsager cross-transport phenomena in the stability of fluid layers heated from below or above has been the subject of intense research in the past decade. Recently, interest has focused on the importance of heat and mass cross-transport processes in cylindrical containers [1, 2]. In the present paper we develop a general, albeit linear, stability analysis of the influence of Soret and Dufour effects upon the stability of the motionless steady state with no restriction on the preferred pattern for convective instability. We discuss the role played by the aspect-ratio of the container and delineate the threshold for *axi-* and *asymmetric* convective rolls. The present paper also extends earlier work on binary gas mixtures in infinitely extended horizontal layers [3].

I. LINEAR STABILITY ANALYSIS

We consider a motionless binary fluid mixture in a vertical cylindrical container of height L and diameter $2R$ (Fig. 1). When the initially homogeneous layer is heated from below the Soret effect distributes the components in accordance with the value given to the thermal gradient ($\Delta T/L$, where T denotes temperature) until the mass and heat fluxes balance each other [4]. On the other hand, past a certain threshold the thermal gradient induces enough buoyancy to destabilize the linearly distributed state of rest thus leading to natural convection [5].

For convenience in the description we choose the following scales: unit length R ; unit time R^2/κ , where κ is the thermal diffusivity (thermometric conductivity) of the mixture; velocity $\kappa L/R^2$; temperature ΔT ; concentration (mass fraction) ΔN_1 ; pressure $\rho^m g L$,

* To whom all correspondence should be addressed.

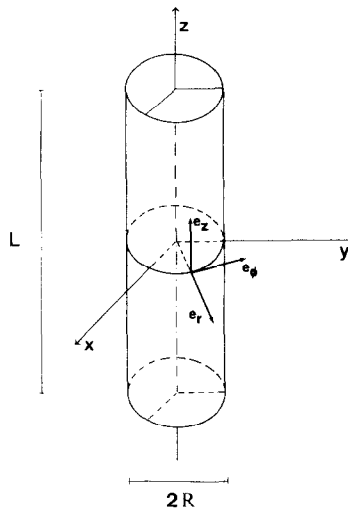


FIG. 1. A sketch of the container. Note that in the main text we have used two different aspect-ratios: $h = L/2R$ and $f = R/L$. $2R$ and L denote diameter and height, respectively. \mathbf{e} denotes a unit vector along a given direction as subscript.

where ρ^m and g denote a reference density and the gravitational acceleration, respectively. We also introduce the following dimensionless groups: aspect-ratio $h = L/2R$; Rayleigh number $\tilde{Ra} = \alpha g \Delta T R^4 / (\nu k L)$, where α is the thermal expansion coefficient and ν is the kinematic viscosity; Prandtl number $P = \nu/\kappa$; (inverse) Lewis number $r_D = D/\kappa$, where D denotes the mass diffusivity; Soret separation or buoyancy factor $S = -\gamma \Delta N_1 / (\alpha \Delta T)$, where γ is the density variation induced by a change ΔN_1 in the mass-fraction of, for example, component one; Dufour number $D_F = +TN_1 D'' \Delta N_1 (\partial \mu_1 / \partial N_1)_{p,T} / \kappa c_p \Delta T$, where D'' is Onsager's Dufour cross-coefficient [4]; μ_1 is the chemical potential of component one that we take as the denser in the mixture. We also take S positive when the denser component migrates to the colder boundary. The superscript m denotes some reference value given to the relevant quantity, say, the value at the bottom surface; c_p is the specific heat at constant pressure.

With the above introduced scales and definitions the thermohydrodynamic evolution of disturbances upon the motionless state of the fluid layer is given by the following set of partial differential equations [3, 6, 7]:

$$\operatorname{div} \mathbf{u} = 0 \quad (1.1)$$

$$P^{-1} \partial \mathbf{u} / \partial t = \tilde{Ra} \operatorname{grad} p / \alpha R \Delta T + \nabla^2 \mathbf{u} + [\tilde{Ra}(1 + S)T + S R a \Omega] \mathbf{e}_z \quad (1.2)$$

$$\partial T / \partial t = (1 + D_F) \nabla^2 T + D_F \nabla^2 \Omega + w \quad (1.3)$$

$$\partial \Omega / \partial t = (r_D - D_F) \nabla^2 \Omega - (1 + D_F) \nabla^2 T \quad (1.4)$$

where $\mathbf{u} = (u, v, w)$ accounts for the 3-dim. velocity field; t denotes dimensionless time; $\Omega = T - \Gamma$ (for convenience we introduce a dimensionless difference

between the temperature and mass-fraction fields) and $\mathbf{e}_z = (0, 0, +1)$.

We restrict consideration to the following accepted realistic boundary conditions (b.c.): rigid walls that are impervious to matter transfer and good heat conductors. We have $\mathbf{u} = 0$, $T = 0$ and $\nabla \Omega \cdot \mathbf{n} = 0$ at $Z = \pm h$ and $R = 1$, where \mathbf{n} denotes the outward unit normal vector to the horizontal or vertical boundaries of the cylinder.

2. FORMAL SOLUTION OF THE STABILITY PROBLEM: ARBITRARY MODES OF CONVECTION

The system of equations (1.1)–(1.4) has been solved using the Galerkin method [7, 8]. With \mathbf{u} now denoting the velocity field in cylindrical coordinates (Fig. 1), $\mathbf{u} = (u_r, u_\phi, u_z)$, we set

$$u_r = z(h^2 - z^2)u(r) \cos n\phi, \quad (2.1)$$

$$u_\phi = z(h^2 - z^2)v(r) \sin n\phi, \quad (2.2)$$

$$u_z = \frac{1}{4}(h^2 - z^2)^2 w(r) \cos n\phi. \quad (2.3)$$

Note that we have assumed periodicity along the ϕ coordinate and that the radial parts satisfy the continuity equation. We have

$$u(r) = -[J'_n(kr) - J'_n(k)r^{n+1}] / k J_n(k), \quad (2.4)$$

$$v(r) = [J_n(kr)/r - J_n(k)r^{n+1}]n/k^2 J_n(k), \quad (2.5)$$

$$w(r) = J_n(kr)/J_n(k) - r^n \quad (2.6)$$

where k obeys the relation

$$k J''_n(k) = (n+1) J'_n(k) \quad (2.7)$$

and the primed symbols denote derivatives with respect to the argument.

Thus, according to the value given to n we have axisymmetric rolls ($n = 0$), asymmetric rolls ($n = 1$) and higher order modes ($n \geq 2$).

As the chosen trial functions for the velocity field are an exact solution of the continuity equation we use them to generate trial functions for the fields T and Ω [8]. We have

$$T = \theta_1(r)(h^2 - z^2)(5h^2 - z^2) \cos n\phi, \quad (2.8)$$

$$\Omega = \theta_2(r) \cos n\phi \cos(z\delta_2) \quad (2.9)$$

where

$$\theta_1(r) = [11/248 \delta_1^2(k^2 + \delta_1^2)] [\delta_1^2 J_n(kr)/J_n(k) + k^2 I_n(\delta_1 r)/I_n(\delta_1) - (k^2 + \delta_1^2)r^n]. \quad (2.10)$$

$$\theta_2(r) = AJ_1(kr)/J_1(k) + BI_n(\delta_2 r) + Cr^n \quad (2.11)$$

with

$$A = 12h^4/\pi^4(k^2 + \delta_2^2), \quad (2.12)$$

$$B = [1/\delta_2 I'_n(\delta_2)] [12h^4/\pi^4 \delta_2^2(k^2 + \delta_2^2)] \times [n(k^2 + \delta_2^2) - k\delta_2^2 J'_n(k)/J_n(k)], \quad (2.13)$$

$$C = -12h^4/\pi^4 \delta_2^2, \quad (2.14)$$

$$\delta_1^2 = 153/62h^2 \quad (2.15)$$

and

$$\delta_2 = \pi/h. \quad (2.16)$$

The functions J_n and I_n refer to the Bessel and modified Bessel functions [10].

Then the critical Rayleigh number for the onset of (steady) convection is given by the following equation

$$\tilde{Ra}^c = - \langle \mathbf{u} \cdot \nabla^2 \mathbf{u} \rangle / [\langle w T \rangle (1 - D_F/r_D)(1 + S) / (1 + D_F) + \langle w \Omega \rangle S/r_D] \quad (2.17)$$

where the bracket denotes the following scalar product

$$\langle fg \rangle = \int fg \, dV \quad (2.18)$$

with f and g two arbitrary solutions of the problem and the integration goes over the whole cylinder (volume, V).

A general expression for \tilde{Ra}^c can be given for an arbitrary value of n . However, we shall discuss here results for the $n = 0$ (axisymmetric) and $n = 1$ (asymmetric) modes.

We have

$$n = 0$$

$$\langle \mathbf{u} \cdot \nabla^2 \mathbf{u} \rangle = - (h^5/630) [189 + 24h^2k^2 + 4h^4k^4] \quad (2.19)$$

$$\langle w T \rangle = [121h^9k^2/19530\delta_1^2(k^2 + \delta_1^2)^2][\delta_1^4 + \delta_1^2k^2 + 4k^2 - 8k^2I_1(\delta_1)/\delta_1I_0(\delta_1)] \quad (2.20)$$

$$\langle w \Omega \rangle = [18h^9k^2/\pi^8\delta_2^2(k^2 + \delta_2^2)] [\delta_2^4 + k^2\delta_2^2 - 4k^2 + 2k^2\delta_2I_0(\delta_2)/I_1(\delta_2)]. \quad (2.21)$$

$$n = 1$$

$$\begin{aligned} \langle \mathbf{u} \cdot \nabla^2 \mathbf{u} \rangle &= - (4h^5/2835k^4) [2h^4k^4(k^4 + k^2 - 20) \\ &+ 3h^2(4k^6 - k^4 - 112k^2 + 64) \\ &+ 21(4k^4 + k^2 - 104)], \end{aligned} \quad (2.22)$$

$$\begin{aligned} \langle w T \rangle &= (121h^9/87885) [k^2\delta_1^4(k^2 + \delta_1^2)^2]^{-1} \\ &\times [72k^6 + 2\delta_1^4k^2(k^4 - 2k^2 - 44) \\ &+ \delta_1^6(2k^4 - k^2 - 64) - 36\delta_1k^6I_0(\delta_1)/I_1(\delta_1) \\ &+ 9k^6\delta_1^2], \end{aligned} \quad (2.23)$$

$$\begin{aligned} \langle w \Omega \rangle &= [4h^4/\pi^8(k^2 + \delta_2^2)^2\delta_2^4] \{\delta_2^6(2k^4 - k^2 - 64) \\ &+ \delta_2^4k^2(2k^4 - 4k^2 - 88) - 3k^4\delta_2^2(k^2 + 8) \\ &+ 4k^2(3k^2 + 2\delta_2^2 + \delta_2^2k^2) \\ &+ [(k^2\delta_2^2 + 6k^2 + 2\delta_2^2)I_1(\delta_2) - 3k^2I_0(\delta_2)] \\ &\times [\delta_2I_0(\delta_2) - I_1(\delta_2)]^{-1}\}. \end{aligned} \quad (2.24)$$

3. DISCUSSION OF RESULTS AND COMPARISON WITH EXPERIMENTAL DATA

The critical Rayleigh number for the onset of convective instability, \tilde{Ra}^c , is a rather involved function of the parameters of the problem, S , D_F , r_D and h . For illustration we give some of the results found. Figure 2

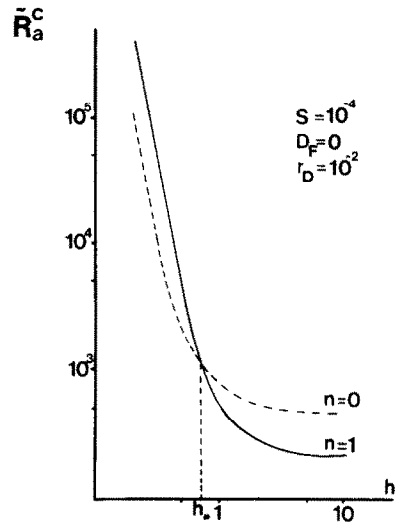


FIG. 2. Critical Rayleigh number for axi- and asymmetric modes of convection ($n = 0$ and $n = 1$, respectively) as a function of aspect-ratio, h , and given values of Soret and Lewis numbers ($S = 10^{-4}$, $r_D = 10^{-2}$). Note the cross-over of the two modes at $h = h^* = 0.74$. Different values of S and r_D do not alter the qualitative picture.

provides the critical Rayleigh number as a function of the aspect-ratio. It appears that at a certain value of h , called h^* , around 0.7, there is a cross-over between the axi- and asymmetric modes of convection as already happens with single-component liquid layers [8]. Past h^* the taller the cylinder the greater is the tendency towards asymmetric cells.

Figure 3 illustrates the rather minor role played by the Dufour effect as already noted in the stability analysis of infinitely extended horizontal layers [3].

Figures 4 and 5 provide a comparison between theory and experiment. This corresponds to the mixtures Xe : He and Xe : Ar, respectively. For the sake of completeness we report the values of the first-order Galerkin calculation using two normalization factors, one corresponds to a mere displacement of the curve to fit the experimental data at vanishing molar fraction of Xe and the other to a weighted correction factor of 200 (the experimental value) over 247.25 (our theoretical result). The former fit provides quite a satisfactory description of the experimentally available data [2].

Figure 6 also compares theory with experiment using the parameter $\Psi = S(1 + D_F)/r_D(1 + S)(1 - D_F/r_D)$, introduced in ref. [11]. The peaks shown in this curve follow the variation of Ψ with the mass-fraction of Xe as reported in ref. [2] thus illustrating a difficulty with the use of such an involved combination of parameters. There are no peaks in a plot of critical Rayleigh numbers vs Soret separation, S . Moreover, the curve for infinitely extended layers lies well below the corresponding curve for a bounded cylinder which indicates the expected stabilizing effect of the lateral boundaries [8].

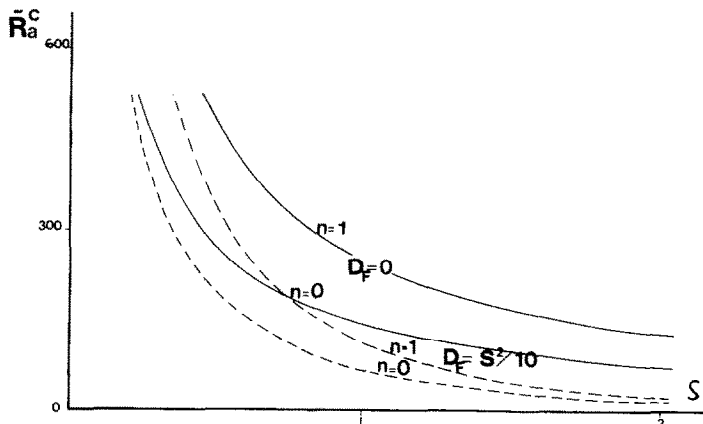


FIG. 3. An illustration of the role of Dufour effect on the stability analysis. Note that at vanishing Soret coefficient all curves must cross the vertical axis at the critical Rayleigh number for the onset of convection in single-component layers. Different values of the aspect-ratio (here $h = 0.5$) do not alter the qualitative picture. Solid and broken lines respectively correspond to vanishing and non-vanishing Dufour coefficient.

4. ALTERNATIVE DESCRIPTION OF THE PROBLEM: THE CASE OF AXYSYMMETRIC CONVECTION

When restriction to axisymmetric modes of convection is made a more suitable set of scales is the following: vertical length L ; horizontal length R ; pressure $\rho^m \nu k Ra^{1/2}$; velocity $\kappa Ra^{1/2}/L$ where now the Rayleigh number is $Ra = \alpha g L^3 \Delta T / \kappa v$ and the aspect ratio $f = R/L$. All other scales are the same as defined earlier in section 2. Then the thermohydrodynamic evolution of disturbances upon the initially motionless steady state is governed by the following set of equations:

$$f^{-1} \partial u / \partial r + (rf)^{-1} u + \mathbf{e}_z \partial (\mathbf{u} \cdot \mathbf{e}_z) / \partial z = 0, \quad (4.1)$$

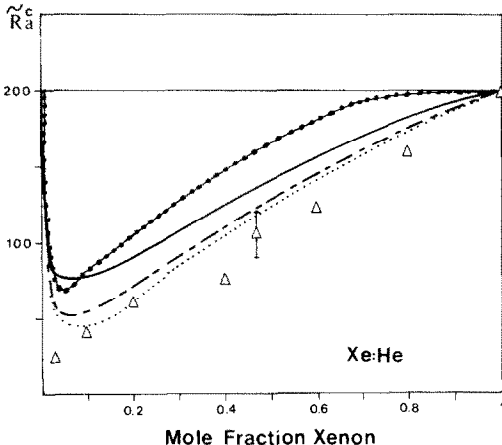


FIG. 4. Comparison between theory and experimental data for the Xe:He mixture: ----- infinitely extended horizontal layer (results from refs. [3] and [11] as reported in ref. [2]. The latter authors in fact plot the quantity $(200/1707) (RaS/r_D \Psi)$; --- infinitely extended horizontal layer (results from ref. [3] and [11] when the critical Rayleigh number \tilde{Ra}^c is used); —— this work (first-order Galerkin calculation) normalized with the factor 200/247.25 (experimental vs theoretical values at vanishing Xe mole fraction); ... this work (first-order Galerkin calculation) corrected with the systematic deviation between theory and experiment at vanishing Xe mole fraction; Δ , experimental data as reported in ref. [2].

$$f^{-1} \partial p / \partial r - f^{-2} \partial [(1/r) \partial (ru)] / \partial r - \partial^2 u / \partial z^2 + P^{-1} \partial u / \partial t = 0, \quad (4.2)$$

$$\begin{aligned} \partial p / \partial z - Ra^{1/2} T - (rf)^{-1} \partial [r \partial (\mathbf{u} \cdot \mathbf{e}_z) / \partial r] / \partial r \\ - \partial^2 (\mathbf{u} \cdot \mathbf{e}_z) / \partial z^2 - SRa^{1/2} \Gamma + P^{-1} \partial (\mathbf{u} \cdot \mathbf{e}_z) / \partial t = 0, \end{aligned} \quad (4.3)$$

$$\begin{aligned} (rf)^{-1} \partial (r \partial T / \partial r) / \partial r + \partial^2 T / \partial z^2 + Ra^{1/2} (\mathbf{u} \cdot \mathbf{e}_z) \\ + D_F [(rf)^{-1} \partial (r \partial \Gamma / \partial r) / \partial r + \partial^2 \Gamma / \partial z^2] \\ - \partial T / \partial t = 0 \end{aligned} \quad (4.4)$$

$$\begin{aligned} (r_D / rf^2) \partial (r \partial \Gamma / \partial r) / \partial r + r_D \partial^2 \Gamma / \partial z^2 + Ra^{1/2} (\mathbf{u} \cdot \mathbf{e}_z) \\ - S [(rf)^{-1} \partial (r \partial T / \partial r) / \partial r + \partial^2 T / \partial z^2] \\ - \partial \Gamma / \partial t = 0 \end{aligned} \quad (4.5)$$

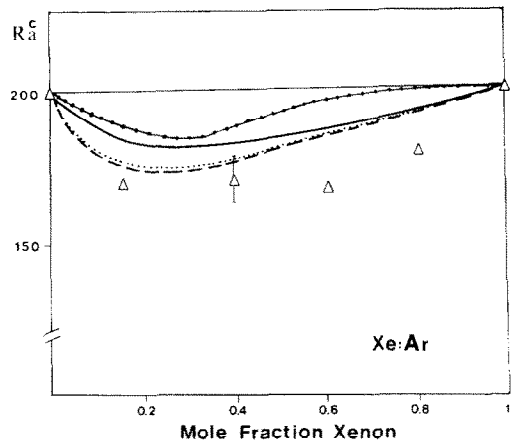


FIG. 5. Comparison between theory and experimental data for the Xe:Ar mixture: ----- infinitely extended horizontal layer (results from refs. [3] and [11] as reported in ref. [2]; --- infinitely extended horizontal layer when \tilde{Ra}^c is used; —— this work (first-order Galerkin calculation) normalized as in the preceding figure; ... this work (first-order Galerkin calculation) normalized as in the preceding figure with the systematic deviation at vanishing Xe mole fraction; Δ , experimental data as reported in ref. [2].

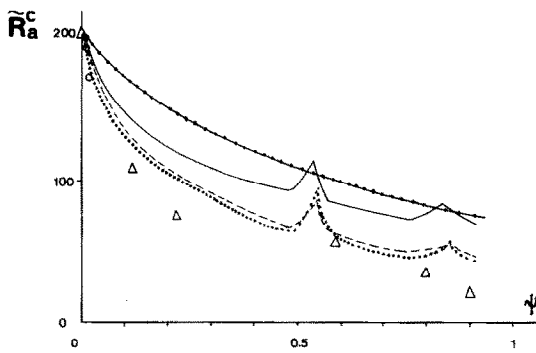


FIG. 6. Comparison between various theoretical predictions and experimental data. The parameter $\Psi = S(1 + D_F)/r_D(1 + S)(1 - D_F/r_D)$ was introduced in ref. [11] and its values have been tabulated in ref. [2]. \cdots , infinitely extended horizontal layer (results from refs. [3] and [11] as reported in ref. [2]; \cdots , infinitely extended horizontal layer when the Rayleigh number \tilde{Ra}^c is used; \cdots , this work normalized with the factor 200/247.25; \cdots , this work corrected for a systematic deviation at vanishing Xe mole fraction; \circ , Δ , experimental data as reported in ref. [2].

where we have retained Γ for the value of the disturbance upon the field $N_1 \cdot \mathbf{u} = (u, 0, w)$ accounts for the velocity.

For axisymmetric convection we take the following trial functions

$$u \equiv U J_1(\alpha r)z(z - 1)(z - 0.5), \quad (4.6)$$

$$w \equiv W J_0(\alpha r)z(z - 1), \quad (4.7)$$

$$T \equiv \Theta J_0(\alpha r)z(z - 1), \quad (4.8)$$

$$\Gamma \equiv \tilde{\Gamma} J_0(\alpha r), \quad (4.9)$$

$$p \equiv \tilde{P} J_0(\alpha r)z \quad (4.10)$$

where α satisfies the relation $J_0(\alpha) = 0$.

Again, we consider rigid, impervious and heat conducting boundaries. The problem has been solved using the Galerkin method [8, 9]. Sufficient conditions

for convective instability correspond the following critical Rayleigh number

$$\begin{aligned} Ra^c = & \{(200f^2/7\alpha^2)[(1 - \alpha^2/2)/f^2 - 21][5D_F(\alpha^2/f^2 \\ & + 12)\alpha^2/f^2 + 6(\alpha^2/f^2 + 10)(\alpha^2/f^2 + 2)] \\ & - 6(\alpha^2/f^2 + 10)^2(\alpha^2/f^2 + 2) \\ & - 5D_F(\alpha^2/f^2 + 12)(\alpha^2/f^2 + 10)\alpha^2/f^2\} \\ & \times [6(\alpha^2/f^2 + 2) + 5S(\alpha^2/f^2 + 10)/r_D \\ & + 5S(\alpha^2/f^2 + 12) - 5D_F\alpha^2/r_Df^2]^{-1}. \quad (4.11) \end{aligned}$$

The results obtained with equation (4.11) are described in the following section. It suffices here to note that with vanishing Soret and Dufour coefficients and infinitely large values of f we obtain a critical Rayleigh number of 1884.3 and a critical wavenumber of 3.22 which compare rather well with the more accurate results of 1707 and 3.14 already known in the literature.

5. AXISYMMETRIC MODE OF CONVECTION: DISCUSSION OF RESULTS

Table 1 gives the predictions concerning wavenumber, i.e. the number of axisymmetric rolls and critical Rayleigh number as functions of the aspect-ratio, $f = R/L$ and Soret separation. The latter parameter plays a strongly destabilizing effect whereas low values of the aspect-ratio rather tend to stabilize the layer. For the sake of completeness we also provide a comparison of our predictions with some other results known in the literature, theoretical [12] and experimental [13]. The agreement obtained is valid enough to encourage further experimental studies of convection in cylinders of varying aspect-ratio and adequate choice of relevant boundaries.

Acknowledgements—The authors acknowledge fruitful discussions with Professor E. L. Koschmieder and Dr. P. L. Garcia-Ybarra. This research has been sponsored by the Stiftung Volkswagenwerk.

Table 1. Number of axisymmetric rolls as a function of aspect-ratio, $f = R/L$. Large values of f approximate the infinitely extended horizontal layer. Note that for given aspect-ratio the Soret effect induces a change of wavenumber.

f	Ra^c	S		
		0	0.01	0.1
		Rolls	Rolls	Rolls
1	2975	1	1467	1
4	1902	3	779	3
7	1894	6	779	5

Table 2. Critical Rayleigh number and number of axisymmetrical rolls as a function of aspect-ratio and vanishing Soret and Dufour effects. The second and third columns account for results obtained respectively with sections 4 and 2. Column 3 refers to results due to Charlson and Sani [12]. The last column gives the findings of Koschmieder [13], albeit for insulating lateral walls.

f	Ra^c	Rolls	Ra^c	Rolls	Ra^c	Rolls[12]	Rolls[13]
9.8	1887	10	2213	10	1714.6	10	10
10.3	1884	10	2216	10	1713.9	10	11
12.9	1886	13	2215	13	1711.8	13	13

REFERENCES

1. M. G. Velarde and P. L. García-Ybarra, A model describing Soret diffusion and convective instability in a closed vertical column, *J. Non-Equilib. Thermodyn.*, **7** (1982).
2. J. R. Abernathey and F. Rosenberger, Soret diffusion and convective stability in a closed vertical cylinder, *Phys. Fluids* **24**, 377–381 (1981).
3. P. L. García-Ybarra and M. G. Velarde, The role of Soret and Dufour effects on the stability of a binary gas layer heated from below or above, *Geophys. Astrophys. Fluid Dyn.* **13**, 83–94 (1979).
4. S. R. de Groot and P. Mazur, *Non-equilibrium Thermodynamics*. North Holland, Amsterdam (1962).
5. M. G. Velarde and Ch. Normand, Convection, *Sci. Amer.* **243**, 92–108 (1980).
6. R. S. Schechter, M. G. Velarde and J. K. Platten, The two-component Bénard problem, *Adv. Chem. Phys.* **26**, 256–301 (1974).
7. For a detailed discussion of the Oberbeck–Boussinesq approximation see R. Pérez-Cordón and M. G. Velarde, On the (nonlinear) foundations of Boussinesq approximation, *J. Phys. Paris* **36**, 591–601; M. G. Velarde and R. Pérez-Cordón, On the (nonlinear) foundations of Boussinesq approximation. Viscous dissipation and large cell gap effects, *J. Phys. Paris* **37**, 176–180 (1976).
8. G. Z. Gershuni and E. M. Zhukhovitskii, *Convective Stability of Compressible Fluids*. Ketterpress Enterprises–Wiley, Jerusalem (1976).
9. B. A. Finlayson, *The Method of Weighted Residuals and Variation Principles*. Academic Press, New York (1972).
10. M. Abramowitz and I. A. Stegun, *Handbook of Mathematical Functions*. Dover, New York (1972).
11. D. Gutkowicz-Krusin, M. A. Collins and J. Ross, Rayleigh–Bénard instability in nonreactive binary fluids, *Phys. Fluids* **22**, 1443–1450 (1979).
12. G. S. Charlson and R. L. Sani, Thermoconvective instability in a bounded cylindrical fluid layer, *Int. J. Heat Mass Transfer* **13**, 1479–1496 (1970); G. S. Charlson and R. L. Sani, On thermoconvective instability in a bounded cylindrical fluid layer, *Int. J. Heat Mass Transfer* **14**, 2157–2160 (1971).
13. For a review see E. L. Koschmieder, Bénard convection, *Adv. Chem. Phys.* **26**, 177–212 (1973).

CONVECTION DE BÉNARD DANS DES CYLINDRES POUR UN FLUIDE BINAIRE

Résumé—On considère un mélange binaire (gaz ou liquide) dans un cylindre vertical chauffé par le bas. Des conditions suffisantes sont données pour l'instabilité permanente thermoconvective. On considère des modes de convection à la fois axi- et asymétriques. Les prévisions théoriques sont comparées aux données expérimentales disponibles.

ZWEIKOMPONENTEN-BÉNARDKONVEKTION IN ZYLINDERN

Zusammenfassung—Es wird ein nicht reagierendes binäres (Gas- oder Flüssigkeits-) Gemisch in einem von unten beheizten vertikalen Zylinder betrachtet. Ausreichende Voraussetzungen für stetige thermokonvektive Instabilität sind gegeben. Es werden sowohl achsensymmetrische als auch unsymmetrische Formen der Konvektion betrachtet. Die Aussagen der theoretischen Berechnungen werden mit den vorhandenen experimentellen Daten verglichen.

ДВУХКОМПОНЕНТНАЯ КОНВЕКЦИЯ БЕНАРА В ЦИЛИНДРАХ

Аннотация—Рассматривается нереагирующая бинарная (газовая или жидкостная) смесь в вертикальном нагреваемом снизу цилиндре. Приводятся условия достаточности для стационарной термоконвективной неустойчивости. Исследуются как симметричные, так и асимметричные режимы конвекции. Результаты теоретических расчетов сравниваются с имеющимися экспериментальными данными.